

PACS numbers: 06.60.Jn; 85.60.Ha; 41.75.Fr; 41.85.–p
DOI: 10.1070/QE2015v045n05ABEH015775

On some limitations on temporal resolution in imaging subpicosecond photoelectronics

M.Ya. Schelev, S.V. Andreev, D.E. Greenfield, V.P. Degtyareva, I.A. Kopaev, M.A. Monastyrskiy

Abstract. **Numerical modelling is used to analyse some effects restricting the enhancement of temporal resolution into the area better than 100 fs in streak image tubes and photoelectron guns. A particular attention is paid to broadening of an electron bunch as a result of Coulomb interaction. Possible ways to overcome the limitations under consideration are discussed.**

Keywords: *subpicosecond photoelectronics, temporal resolution, Coulomb interaction.*

1. Introduction

At the turn of the 1980s and later, along with active development of time-analysing electron-optical converters (streak image tubes) with picosecond temporal resolution, a significant number of publications appeared, dedicated to physical limitations on enhancing the temporal resolution to the values less than 1 ps. A special place among them is occupied by the research associated with the analysis of space charge effects in streak image tubes with static focusing. One can distinguish papers [1–9], in which, along with the design of new, sometimes very advanced streak image tubes, a variety of approximate analytical models are offered or direct numerical simulation of the Coulomb interaction contribution to spatial-temporal resolution and dynamic range in streak image tubes is carried out. It should be noted that the scope of applicability of the approximate analytical models for the solution of the Coulomb interaction problem is rather limited; moreover, the models being often proposed (for example, those based on the Child–Langmuir law for dense stationary electron beams) do not adequately fit the sophisticated dynamic structure of the problem in question.

Numerical simulation, which has in many respects replaced the analytical models, represents a more powerful and versatile tool. In this regard, it is important to emphasise the essential peculiarity of the problem, namely the fact that Coulomb interaction in a picosecond electron bunch is commonly by 5–6 orders of magnitude less than the external electric field that accelerates and focuses the bunch. This makes very problematic 'frontal' application of an overwhelming majority of the well-known software packages (see, e.g., [10–13]) aimed at solving the many-particle Coulomb dynamics problem. In our case, the 'computational noise' associated with numerical calculation of external fields in the systems with a complex geometry of electrodes and also with direct numerical integration of the equations of charged particle motion may completely 'muffle' the sophisticated space-charge effects. To distinguish the respective 'small terms' in the motion equations with an adequate precision, the development of specialised software based on the perturbation theory is required.

In the present paper, this issue is the main topic of discussion, along with a discussion of other limitations arising in advancing the temporal resolution of streak image tubes to the threshold of 100 fs and smaller.

M.Ya. Schelev, S.V. Andreev, V.P. Degtyareva, I.A. Kopaev, M.A. Monastyrskiy A.M. Prokhorov General Physics Institute, Russian Academy of Sciences, ul. Vavilova 38, 119991 Moscow, Russia; e-mail: m.schelev@ran.gpi.ru;
D.E. Greenfield ThermoFisher Scientific (Bremen) GmbH, Hanna-Kunath-Str. 11, 28199 Bremen, Germany; e-mail: dmitry.grinfeld@thermofisher.com

Received 29 January 2015; revision received 06 February 2015
Kvantovaya Elektronika **45** (5) 455–461 (2015)
Translated by M.A. Monastyrskiy

2. Development of specialised software for solving the Coulomb dynamics problems on the basis of perturbation theory

As shown in [14], the calculation of charged particle trajectories in the presence of a space charge treated as a perturbation can be efficiently implemented by means of a decomposition of the basic Lorentz equation

$$\frac{\mathrm{d}^2\boldsymbol{r}}{\mathrm{d}t^2} = \frac{e}{m}\left(-\nabla\Phi + \frac{\mathrm{d}\boldsymbol{r}}{\mathrm{d}t}\times\boldsymbol{B}\right) - \frac{e}{m}\nabla\Phi_{\mathrm{C}} \tag{1}$$

into two interrelated equations, one of which only contains the external electric and magnetic fields, Φ and $\boldsymbol{B}$, whilst the right-hand side of the other (a drift equation in the space of initial parameters) is only determined by Coulomb interaction $\nabla\Phi_{\mathrm{C}}$ between charged particles. Here, e and m are the charge and mass of electron.

The Coulomb potential Φ_{C} satisfies the Poisson equation

$$\Delta\Phi_{\mathrm{C}} = 4\pi\rho \tag{2}$$

with appropriate boundary conditions on the field-generating electrodes, while the charged particle density ρ is determined by the particle coordinates at a given time moment.

The above-mentioned drift equation appears as

$$\frac{\mathrm{d}\xi(t)}{\mathrm{d}t} = \left\| \frac{\partial(\boldsymbol{r},\dot{\boldsymbol{r}})}{\partial(\xi_1\ldots\xi_6)} \right\|^{-1}(t,\xi)\begin{bmatrix} 0 \\ -(e/m)\nabla\Phi_{\mathrm{C}} \end{bmatrix}, \tag{3}$$

where $\xi \in \Xi$ is the vector of initial parameters for the respective 'unperturbed' aberrational trajectories calculated by

neglecting Coulomb interaction. A general perturbed solution is constructed in the form of a nonlinear superposition

$$r(t,\xi_0) = r_{\text{aber}}(t,\xi(t,\xi_0)), \tag{4}$$

which corresponds to the generalised method of varying the initial conditions in analytical mechanics [15] (Fig. 1). Thus, this approach makes possible the active application of precise aberrational methods to the calculation of charged particle trajectories with regard to Coulomb interaction.

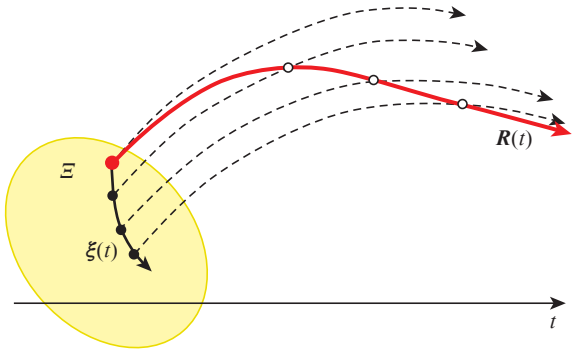

Figure 1. Scheme for calculating the charged particle trajectories with Coulomb interaction treated as a perturbation. Dashed lines show the unperturbed aberrational trajectories of the bunch, calculated by neglecting the space charge; $\xi(t)$ is the solution of (3) in the space of initial parameters, and $\boldsymbol{R}(t)$ is the true trajectory calculated with account for Coulomb interaction.

One of the most important aspects of the procedure under discussion is calculating the Coulomb field of moving charged particles at each step of integrating the motion equations. To do this, we use a modified Barnes–Hut algorithm [16] borrowed from celestial mechanics and adapted to the problems of charged particle optics.

The Barnes–Hut algorithm consists in a tree-type grouping of charged particles, and, within the framework of the modification used here, possesses the computational complexity of $O(N\lg N)$, in contrast to the computational complexity of $O(N^2)$ being characteristic of the direct calculation of the Coulomb sums describing the pair-wise interaction (N is the number of interacting electrons in the charged cloud). A geometric interpretation of the algorithm's scheme is shown in Fig. 2.

An essential element of solving the Coulomb dynamics problems in charged particle optics is the calculation of the 'mirror image' induced by the interaction of a bunch of charged particles with the nearby electrodes. Such a field may cause a significant perturbation of the charged particle trajectories in various problems of corpuscular optics (for example, in the process of electron emission from the photocathode surface or during the passage of an electron bunch in the vicinity of deflecting plates of the linear sweep system). Similar problems also arise in mass-spectrometry of dense ion bunches [17].

We have developed an algorithm that ensures adaptive calculation of the 'mirror-image' field in the process of the bunch motion, depending on the bunch proximity to certain electrodes of a corpuscular-optical system. That algorithm is implemented as a separate programme module of the MASIM 3D package [18].

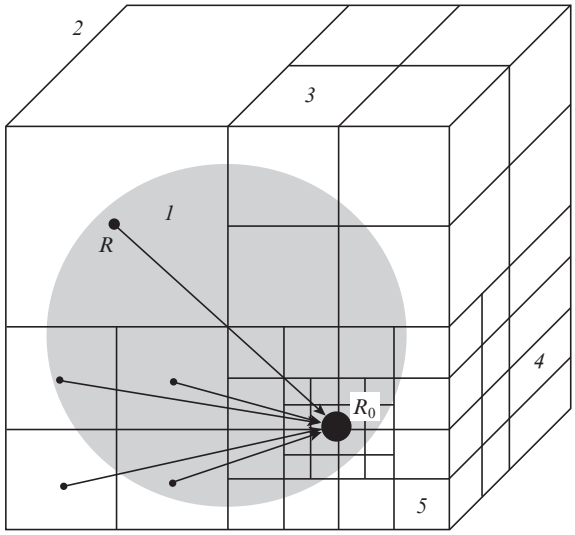

Figure 2. Geometric interpretation of the algorithmic scheme of the modified Barnes–Hut method:
(*1*) cloud of charged particles; (*2*) cube of minimal size, containing the cloud; (*3–5*) cells of different branches of the 'tree' of particles, generated by the algorithm.

The developed algorithms and relevant software have been thoroughly tested using a specially designed set of model problems with strict analytical or quasi-analytical solutions. Due to the limited scope of this paper, the results of test experiments will be presented in a separate publication.

3. Coulomb broadening of electron bunches in subpicosecond streak image tubes and photoelectron guns

As mentioned in the Introduction, the bunch's space charge is one of the main factors limiting the ultimate temporal resolution in streak image tubes. In this Section, we will focus on the analysis of the computer simulation results of the Coulomb broadening of electron bunches in subpicosecond streak image tubes and photoelectron guns, obtained using the above-mentioned software.

Figure 3 shows a schematic of a typical streak image tube with electrostatic focusing and linear image sweep. A photoelectron bunch (*1*) produced by excitation of the photocathode by a laser pulse is accelerated between the photocathode and fine-structure mesh (*2*), falls into to the focusing field governed

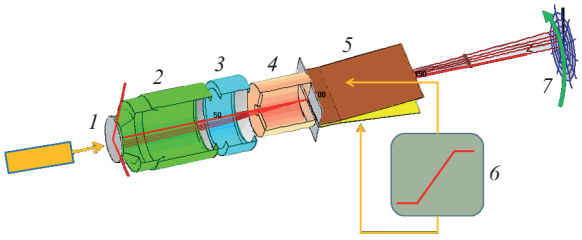

Figure 3. Structure of electrodes of a streak image tube with linear sweep:
(*1*) photocathode; (*2*) fine-structure accelerating mesh; (*3*) focusing electrode; (*4*) anode; (*5*) dynamic deflection system; (*6*) sweep pulse generator; (*7*) image receiver (phosphor screen or CCD camera).

by the electrode (*3*), passes through the aperture of the accelerating anode cylinder (*4*) and undergoes a linear sweep in the dynamic deflection system (*5*) controlled by the pulse sweep generator (*6*). The time-swept spatial electron image of the bunch is recorded on the image receiver (*7*).

Figure 4 shows a typical pattern of focusing of the electron bunches in streak image tubes with static focusing. Clearly visible is the image curvature caused by the difference in focusing conditions for paraxial and off-axis electron bunches. Figure 5 shows the behaviour of electron bunches in the linear sweep mode using a dynamic deflection system.

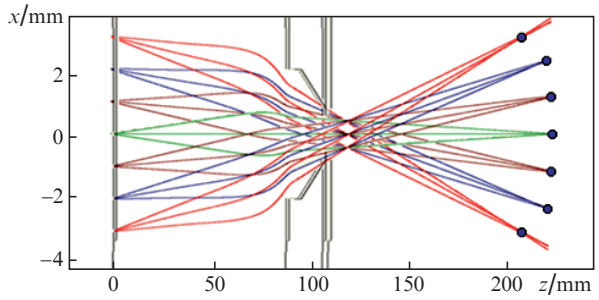

Figure 4. (Colour online) Focusing of electron bunches in the static mode.

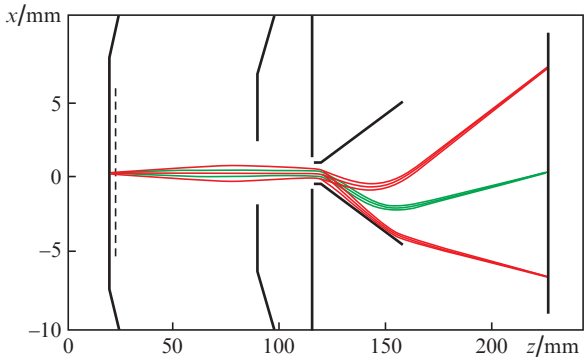

Figure 5. (Colour online) Electron bunches in the linear sweep mode.

Thus, the streak image tube, by means of performing the 'laser pulse → electron beam → electronic image' double conversion, ensures exploring the spatial-temporal structure of the input optical image. It should be emphasised that none of the presently existing analogues of a streak image tube, based on other physical principles, is capable of performing similar analysis with the same quality, elegance and simplicity. Monograph [19] and references therein make it possible for reader to get acquainted with the history of streak image tube development, unique physical experiments in the field of laser physics and its applications that have been carried out using the streak image tube technique, and, finally, with the state of research in this area and nearest prospects.

Figure 6 displays the dependence of the limiting temporal resolution ΔT on the number N of interacting electrons constituting the bunch in the streak image tube with static focusing. Calculations were carried out with the electric field on the photocathode $E_0 = 3$ kV mm^{-1}, the anode potential $U_a = 12$ kV and the width at the half-maximum of the initial energy distribution of photoelectrons $\Delta\varepsilon = 0.25$ eV.

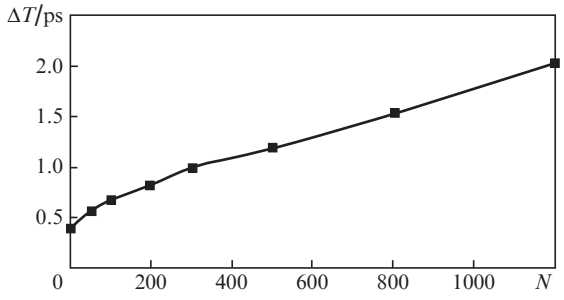

Figure 6. Dependence of the limiting temporal resolution on the number of interacting electrons inside the bunch in the streak image tube with static focusing.

It can be seen from Fig. 6 that the presence of only 300 interacting electrons in the electron bunch have led, in the frame of this numerical experiment, to more than twofold deterioration of temporal resolution (from ~400 fs to 1 ps). Numerical experiments also show that the axisymmetric streak image tubes are the least preferred in terms of contribution of the Coulomb broadening into temporal and spatial resolution. In this case, along with the Coulomb broadening that an electron bunch suffers near the photocathode, there is an additional Coulomb broadening due to the presence of the point of crossover, where the bunch cross section becomes minimal [20].

Another important factor is the initial energy spread of photoelectrons. On the one hand, according to the well-known Zavoisky–Fanchenko formula [21], the physical temporal resolution in a streak image tube can be, in the first approximation, estimated from above as

$$\Delta T \approx \frac{\sqrt{2m}}{eE}\sqrt{\Delta\varepsilon_{\max}}, \qquad (5)$$

where E is the electric field strength near the photocathode, and $\Delta\varepsilon_{\max}$ is the maximal width of the energy distribution of photoelectrons. Formula (5) and more detailed analysis that takes into account the higher-order chromatic aberrations [14] indicate that the smaller the energy spread of photoelectrons, the higher the temporal resolution associated with chromatic aberrations. However, the state of the problems related to the influence of the maximal energy spread $\Delta\varepsilon_{\max}$ on the contribution of Coulomb interaction into the temporal resolution turns out more complicated. Figure 7 shows the electron bunch duration on the image receiver as function of the maximal energy spread $\Delta\varepsilon_{\max}$ of photoelectrons for varying number of interacting electrons in the bunch. It is clearly seen that, for sufficiently large initial energy spread of photoelectrons, Coulomb interaction in the bunch is relatively small, and the temporal broadening of the bunch is mainly determined by chromatic aberrations.

In contrast, at low initial energy spread of photoelectrons, chromatic aberrations are small, but the electron bunch, being sufficiently dense, is heavily exposed to the Coulomb forces, which represent the principal cause of its temporal broadening in this case. The greater the bunch's space charge, the more expressed this effect. It is absent on curve (*4*), where Coulomb interaction of the bunch is neglected, and the temporal broadening of the bunch is determined solely by chromatic aberrations. The results also show that the aspiration of some authors to reduce the initial energy spread of photoelec-

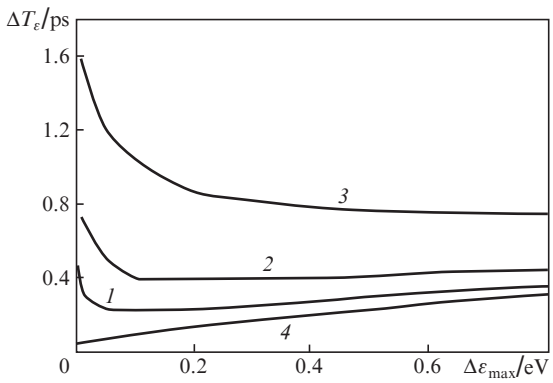

Figure 7. Dependence of the electron pulse duration at the image receiver on the maximal initial energy spread of photoelectrons for $N = (1)$ 74, (2) 220 and (3) 730 [(4) Coulomb interaction is not taken into account]. The emission region on the photocathode represents a circle with a diameter of 0.5 mm, and the initial laser pulse duration is 60 fs [20].

trons with the aim of maximising the temporal resolution may, under certain conditions, lead to the opposite effect.

The Coulomb interaction dynamics of electrons in time-dependent electric fields, and hence the mechanism of space charge contribution to the temporal broadening differ from those in stationary focusing fields that we have considered above. This offers an opportunity to partially compensate for the Coulomb broadening in the nonstationary case. Figure 8 shows the structure of electrodes of a photoelectron gun intended for temporal compression of photoelectron bunches in time-dependent fields as applied to the time-resolved electron diffraction (TRED) method [22], whilst Fig. 9 illustrates the principle of its action (see also [14, 23]).

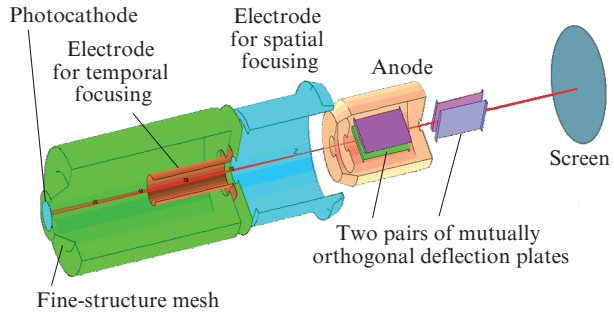

Figure 8. Structure of electrodes of the hybrid photoelectron gun intended for temporal compression of photoelectron bunches [14].

The principle of operation of the photoelectron gun in question is as follows. A femtosecond laser pulse is split into two pulses: one of them excites the photocathode (2) and initiates the photoelectron bunch, while the other passes through the controlled delay line (3), hits the sample (4) and excites in it fast physical processes to be examined by TRED. The photoelectron bunch emitted from the photocathode is accelerated in a strong electric field located between the photocathode and a fine-structure mesh. After passing through the mesh, the electrons fall into a time-dependent electric field generated by the electrode (5), on which the electric pulse generator (8) creates a potential linearly varying in time. The change rate of the time-dependent potential determines the degree of temporal compression of electron bunch (in our

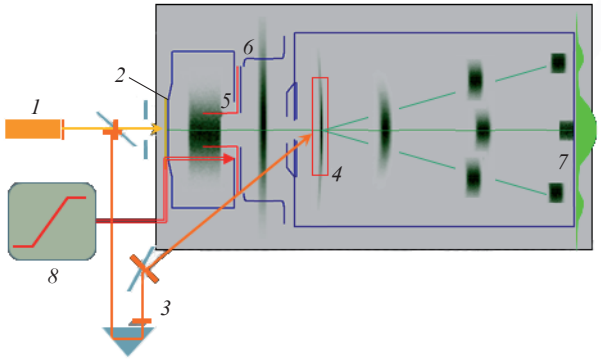

Figure 9. Operating principle of the photoelectron gun with time-dependent electric fields, intended for temporal compression of electron bunches:
(1) laser; (2) photocathode; (3) optical delay line; (4) sample; (5) electrode responsible for temporal focusing; (6) electrode responsible for spatial focusing; (7) image receiver; (8) electric pulse generator. The linear sweep system is not shown; the bunch sizes are deliberately exaggerated.

experiments, this rate constituted several kilovolts per nanosecond). The time-dependent potential is synchronised with the initiating laser pulse to ensure a controlled delay between the bunch emission from the photocathode and the effect on the bunch of the nonstationary electric field responsible for temporal focusing. During the passage of the bunch through the nonstationary electric field area, the difference between the energies of electrons at the leading and trailing edges of the bunch is changed, and the bunch acquires a momentum of longitudinal compression along the main optical axis.

The electric and electrodynamic parameters of the photoelectron gun are optimised so as to ensure the coincidence of the position of the point of maximal longitudinal compression of the electron bunch (temporal focus) with the sample surface, which, in turn, is positioned near the dynamic deflection centre to enable direct measurement of the bunch duration at the temporal focus in the linear sweep mode. In the TRED mode, a diffraction pattern resulted from interaction of the compressed electron bunch with the atomic-molecular structure of the sample, which is excited (with an adjustable delay) by the laser pulse exposure, is formed on the image receiver. In the test mode the sample is removed, and the bunch is swept by the dynamic deflection system over the image receiver surface, thus allowing implementation of the standard streak tube mode to measure the bunch duration at the temporal focus.

Figure 10 shows the dependence of the electron pulse duration in the sample in the photoelectron gun on the amplitude ΔU of the electric pulse providing the temporal focusing at different N. The initial duration of the electron pulse is $\Delta T_0 = 10$ ps, the change rate of the time-focusing electric pulse potential is $dU/dt = 2$ kV ns^{-1}, $E_0 = 3$ kV mm^{-1}, $U_a = 13$ kV and $\Delta\varepsilon = 0.25$ eV.

It is clearly seen that controlling the nonstationary field amplitude ΔU can largely compensate for the Coulomb broadening of the electron bunch at the point of temporal focus. In particular, if the electron bunch contains 3000 electrons, the change in ΔU from 3000 to 3800 V ensures more than a twofold decrease in the compressed pulse duration. Theory and numerical experiments show that for larger values of the change rate dU/dt of the time-focusing potential, this effect becomes still more pronounced.

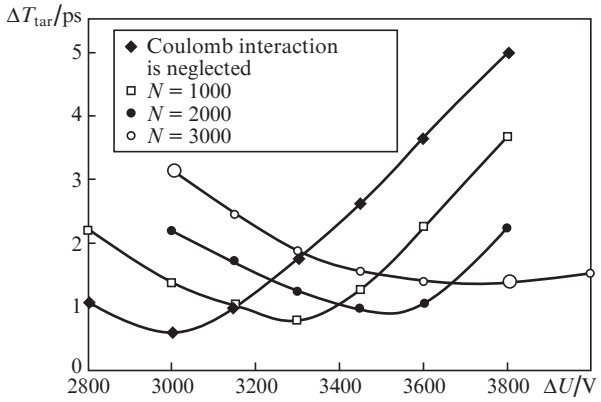

Figure 10. Dependence of the electron pulse duration at the sample in the photoelectron gun on the amplitude ΔU of the electrical pulse providing temporal focusing for different N (see also [14]).

4. Numerical study of the possibility of replacing the near-cathode fine-structure mesh with a narrow slit in the streak image tube of PIF-01 type

The aim of the numerical experiments described below is to investigate the possibility of replacing, in the PIF-01 streak tube, a fine-structure mesh, which provides a high field strength near the photocathode, with an electrode having a narrow rectangular slit (we have analysed the slit dimensions of 1×6 mm) as applied to the 'picosecond dissector' device being now developed in the framework of the Russian Science Foundation Project No. 14-29-00295. The technological advantages of using a slotted accelerating electrode instead of a fine-structure mesh in axisymmetric streak image tubes are well known and have been confirmed by the recent designs developed at Photek and Photonis companies. In this relation, patent [24] is also of certain interest.

However, the practically important question remains open: is it possible to use a slotted electrode instead of the fine-structure mesh, maintaining at the same time high temporal resolution and acceptable spatial resolution in two mutually perpendicular directions?

For computer modelling, the standard PIF-01 geometry (Fig. 11) was used, in which the fine-structure mesh was replaced with a slot electrode having the dimensions of 1×6 mm (Fig. 12). The photocathode curvature radius and electrode potentials were also being varied.

Replacing the fine-structure mesh with a slotted electrode disturbs the axial symmetry, herewith the scattering action of

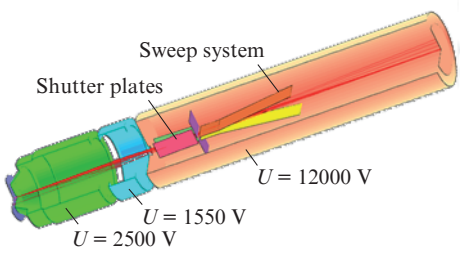

Figure 11. Scheme of the electrodes in the streak image tube of PIF-01 type with a slit near the photocathode.

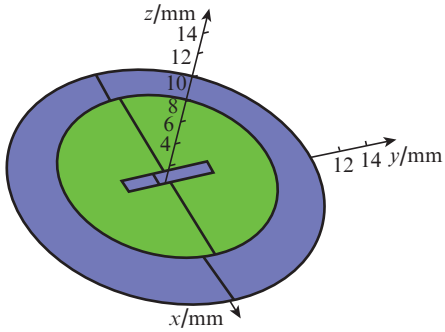

Figure 12. Geometry of the slit with the dimensions of 1×6 mm, which replaces a fine-structure mesh near the photocathode.

the slit in the temporal plane xz (Fig. 13a) leads to a marked paraxial astigmatism. Since the image receiver plane is usually installed in such a way as to provide the best spatial resolution along the temporal axis, the paraxial astigmatism, generally speaking, results in some loss of spatial resolution along the spatial direction (in yz plane). However, the calculations show that the optimal choice of the photocathode's curvature, namely its reduction from 143 mm in the basic streak tube design with a fine-structure mesh down to 80 mm in the streak tube with a slotted electrode, along with corresponding change in the focusing voltages, allows one to substantially compensate for the fall of spatial resolution along the spatial

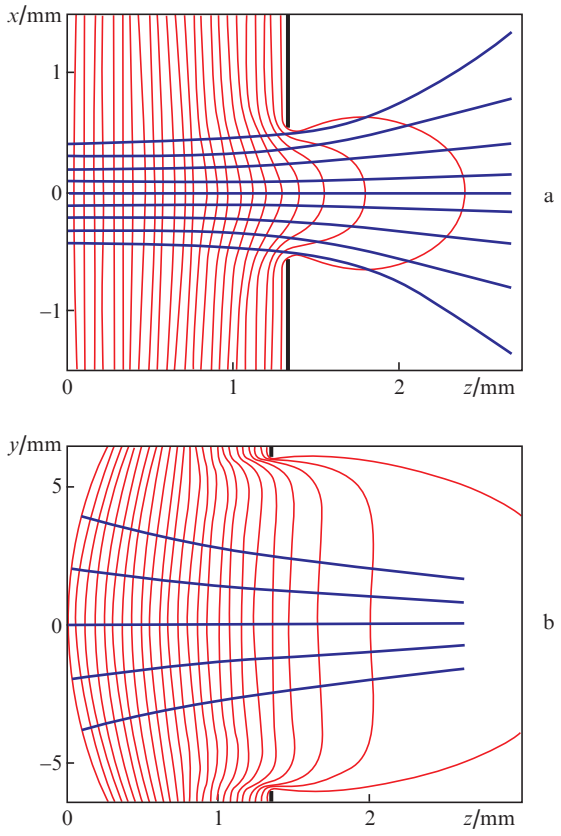

Figure 13. Equipotential lines of the electric field and electron trajectories in the mutually perpendicular planes (a) xz and (b) yz in the photocathode vicinity of the streak image tube with a slit replacing a fine-structure mesh. The scattering effect produced by the slit in the xz plane is clearly seen.

direction. With electron-optical magnification $M_{xz} = 0.75$ in the temporal direction ('across the slit') and electron-optical magnification $M_{yz} = 1.72$ in the spatial direction ('along the slit'), we managed to keep the temporal resolution of about ~1 ps, while ensuring a nearly perfect spatial focusing along the temporal axis and spatial resolution of at least 30 pairs of lines per millimetre along the spatial axis (Fig. 14). The photocathode working area in temporal direction, which is most critical in the problem under consideration, amounted to about 70 μm at the transmittance of ~80%. We should note that our results indicate the excessive categoricity of the statement [24] on the 'extremely low spatial resolution along the spatial axis' in the systems with a slotted electrode located near the photocathode.

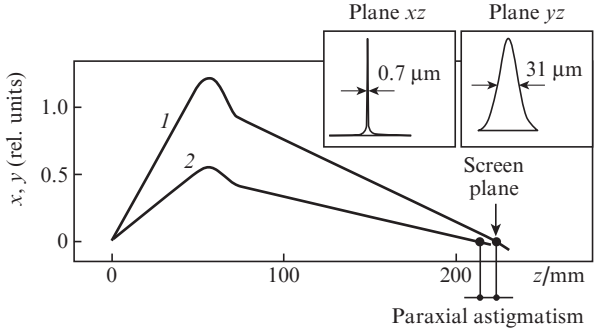

Figure 14. Focusing of electron trajectories forming the Gauss plane in two mutually perpendicular planes *xz* [(*1*) temporal direction] and *yz* [(*2*) spatial direction] in the streak image tube of PIF-01 type with a slit near the photocathode.

Numerical estimates also show that the presence of an extended slit allows one to reduce the Coulomb effects near the photocathode by 3–4 times and thereby to expand the dynamic range of the device.

5. Conclusions

The last decade has shown that overcoming the 100-fs temporal resolution barrier in streak image tubes and photoelectron guns is a more complex problem than previously imagined. It has become clear that a number of extremely complicated physical and engineering problems have to be solved on this way. A detailed analysis of the problem as a whole has been presented in review papers [25–27]; here we touch upon only a few key factors. One of them is the need to increase the electric field strength near the streak tube photocathode up to ~25–30 kV mm^{-1}. As shown in [28], at a sufficiently high field strength near the photocathode ($E \geqslant 8$ kV mm^{-1}), Zavoisky–Fanchenko formula (5) does not accurately describe the electron pulse duration at the image receiver, and therefore taking into account the higher-order chromatic aberrations is required. Of course, the desired field strength cannot be created in static mode because of the risk of electrical breakdown; thus, the development of special electronic schemes for the pulse power supply in the near-cathode region is of profound importance. A positive role here could be played by the replacement of the fine-structure mesh with a slit diaphragm, as discussed above. It is known that, provided the slit diaphragm's electrodes have been properly processed, the gap between the photocathode and the slit diaphragm can have a much greater electric strength than that between the photocathode and the fine-structure mesh. Besides, it seems very promising to use magnetic focusing along with electrostatic acceleration of the bunch, as suggested in [4, 8].

The best result we have experimentally gained in temporal focusing of electron bunches with nonstationary electric fields using the photoelectron gun developed at the Photoelectronics Department, General Physics Institute (GPI) (Figs 8, 9) was temporal compression of an electron bunch from 7 ps down to 280 fs at the time-focusing potential change rate $dU/dt \approx 2$ kV ns^{-1} [23]. Numerical simulations indicate that more substantial progress is only possible by increasing the value of dU/dt at least by an order of magnitude. Of course, if the electron bunch duration on the sample constitutes tens of femtoseconds, Coulomb limitations associated with the permissible number of electrons in the bunch increase significantly, which means that performing the TRED experiments in this case is, apparently, only possible in the mode of accumulation of repetitive processes [29–31].

Finally, we shall briefly touch upon the problem of measuring the femtosecond electron pulse duration. Experiments and numerical simulations show that the applicability of the standard linear sweep technique is currently limited to the duration of about 100 fs. This limitation is mainly due to the scattering effect caused by the fringe fields in the dynamic deflection system. Those fields considerably distort the swept image profile while operating with the required phase sweep speed exceeding the speed of light by 3–5 times. In some cases, the dynamic focusing of swept images can be, at least partially, eliminated at the expense of changing the potentials of focusing electrodes; nonetheless, even in this case, a certain loss in temporal resolution as a rule occurs.

Two approaches are possible here. One of them consists in extending the traditional linear sweep technique to electron pulses of less than 100 fs duration and requires upgrading the dynamic deflection system (in particular, the use of dynamic deflection systems of 'travelling-wave' type [32]). Other approaches to measuring the subpicosecond electron bunch duration, being actively developed at present, are based on the indirect physical methods, such as the method of measuring the spectrum of Auger electrons produced in the interaction of an electron bunch with a sample [33].

Acknowledgements. The authors express their deep gratitude to all the staff members of the Photoelectronics Department, GPI, who to this day provide uninterrupted works in the field of imaging subpicosecond photoelectronics. The work has been carried out in the framework of the Extreme Light Fields and Their Applications programme of the Presidium of the Russian Academy of Sciences and with a financial support of the Russian Science Foundation (Project No. 14-29-00295).

References

1. Kalibjian R. *Proc. SPIE Int. Soc. Opt. Eng.*, **0189**, 452 (1979).
2. Wiedwald J.D., Lerche R.A. *SPIE Annu. Int. Tech. Symp. Opt. Optoelectron. Appl. Sci. Eng.* (San Diego, CA, USA, 1987).
3. Takiguchi Y., Kinoshita K., Suyama M, Inagaki Y., Tsuchiya Y. *Proc. SPIE Int. Soc. Opt. Eng.*, **0693**, 105 (1986).
4. Kinoshita K., Ito M., Suyama M. *Proc. SPIE Int. Soc. Opt. Eng.*, **0981**, 62 (1988).
5. Dooley P., Little V.I., Sim S., Majumdar S. *Proc. SPIE Int. Soc. Opt. Eng.*, **0097**, 80 (1977).
6. Suyama M., Kinoshita K. *Proc. SPIE Int. Soc. Opt. Eng.*, **1032**, 437 (1988).
7. Niu H., Zhang H., Yang Q.L., Liu Y.P., Wang Y.C., Reng Y.A., Zhou J.L. *Proc. SPIE Int. Soc. Opt. Eng.*, **1032**, 472 (1989).

8. Kinoshita K., Ito M., Suyama M. *Proc. SPIE Int. Soc. Opt. Eng.*, **1032**, 441 (1988).
9. Li Ji., Niu H. *Proc. SPIE Int. Soc. Opt. Eng.*, **2869**, 102 (1997).
10. Blackston D., Demmel J., Neureuther A., Wu B. *Proc. SPIE Int. Soc. Opt. Eng.*, **3777**, 228 (1999).
11. Stickel W. *Proc. SPIE Int. Soc. Opt. Eng.*, **2522**, 340 (1995).
12. Mkrtchyan M., Berger S., Liddle J., Harriott L. *Proc. SPIE Int. Soc. Opt. Eng.*, **2522**, 351 (1995).
13. Read F.H., Chalupka A., Bowring N.J. *Proc. SPIE Int. Soc. Opt. Eng.*, **3777**, 184 (1999).
14. Greenfield D., Monastyrskiy M. *Selected Problems of Computational Charged Particle Optics* (Amsterdam: Elsevier Publishers, 2009, AIEP) Vol. 155.
15. Vil'ke V.G. *Teoreticheskaya mekhanika* (Theoretical Mechanics) (Moscow: Izd-vo MGU, 1998) p. 270.
16. Barnes J., Hut P. *Nature*, **324** (4), 446 (1986).
17. Grinfeld D.E., Kopaev I.A., Makarov A.A., Monastyrskiy M.A. *Nucl. Instrum. Methods Phys. Res., Sect. A*, **645** (1), 141 (2011).
18. Greenfield D.E., Monastyrskiy M.A., Tarasov V.A. *Software Demonstrations Abstract Book, 'CPO-7' Int. Conf.* (Cambridge, UK, 2006) p. 23.
19. Schelev M.Ya., Monastyrskiy M.A., Vorobiev N.S., Garnov S.V., Greenfield D.E. *Aspects of Streak Image Tube Photography* (Amsterdam: Elsevier Publishers, 2013, AIEP) Vol. 180.
20. Degtyareva V.P., Monastyrskiy M.A., Tarasov V.A., Schelev M.Ya. *Opt. Eng.*, **37** (8), 2227 (1998).
21. Zavoisky E.K., Fanchenko S.D. *Dokl. Akad. Nauk SSSR*, **108** (2), 218 (1956).
22. Ishchenko A.A., Girichev G.V., Tarasov Yu.I. *Difraktsiya elektronov: struktura i dinamika svobodnykh molekul i kondensirovannogo sostoyaniya veschestva* (Electron Diffraction: Structure and Dynamics of Free Molecules and Condensed Matter) (Moscow: Fizmatlit, 2013) p. 614.
23. Monastyrskiy M.A., Greenfield D.E., Lozovoi V.I., Schelev M.Ya., Serdyuchenko Yu.N. *Optical Memory and Neural Networks (Information Optics)*, **16** (4), 248 (2007).
24. Bad'in L.V., Zyuzin L.N., Pryanishnikov I.G., Safronov S.I., Slavnov Yu.K., Tarasov R.P. Patent of the Russian Federation 2008135532/28 from 01.09.2008. *Bull.* No. 1 (2010).
25. Schelev M.Ya. *Usp. Fiz. Nauk*, **170**, 1002 (2000).
26. Schelev M.Ya. *Kvantovaya Elektron.*, **31** (6), 477 (2001) [*Quantum Electron.*, **31** (6), 477 (2001)].
27. Schelev M.Ya. *Kvantovaya Elektron.*, **33** (7), 609 (2003) [*Quantum Electron.*, **33** (7), 609 (2003)].
28. Ageeva N.V., Andreev S.V., Degtyareva V.P., et al. *Proc. SPIE Int. Soc. Opt. Eng.*, **7126**, 7126 1B, (2008).
29. Fill E., Veisz L., Apolonski A., Krausz F. *New. J. Phys.*, **8**, 272 (2006).
30. Baum P., Zewail A.H. *Proc. Nat. Acad. Sci.*, **103**, 16105 (2006).
31. Wytrykus D., Centurion M., Reckenthaeler P., Krausz F., Apolonski A., Fill F. *Appl. Phys. B*, **96** (2-3), 309 (2009).
32. Monastyrskiy M.A., Drobot V.G., Schelev M.Ya. *Nucl. Instrum. Methods Phys. Res., Sect. A*, **427**, 219 (1999).
33. Reckenthaeler P., Centurion M., Yakovlev V.S., Lezius M., Krausz F., Fill E.E. *Phys. Rev. A*, **77** (4), 042902 (2008).